Citation: Zhongyou Xie, Limin Guo, Cheng Li, et al. Bending crashworthiness of thin-walled square tubes partially filled with metallic foams. *Journal of Harbin Institute of Technology (New Series)*. DOI:10.11916/j.issn.1005-9113.24002.

Bending Crashworthiness of Thin-Walled Square Tubes Partially Filled with Metallic Foams

Zhongyou Xie[1], *Limin Guo*[2], *Cheng Li*[3,*] *and Jianwen Cai*[3]

(*1.School of Architectural Engineering, Tongling University, Tongling 244061, Anhui, China;*
2.School of Science, Changzhou Institute of Technology, Changzhou 213032, Jiangsu, China;
3.School of Automotive Engineering, Changzhou Institute of Technology, Changzhou 213032, Jiangsu, China)

Abstract: Two cross-sectional configurations of thin-walled square tubes partially filled with lightweight metallic foams are proposed, and termed as double-cell configuration partially filled with foam (DC-PF) and double-tube configuration partially filled with foam (DT-PF), respectively. The bending crashworthiness is investigated based on three-point bending tests using finite element ABAQUS/Explicit code. The two key mechanical indicators including Crash Load Efficiency (CLE) and Specific Energy Absorption (SEA) are introduced to evaluate the effect of foams in comparison with empty square tubes and fully filled square tubes. The numerical results show that the two partially filled configurations, especially DT-PF, display dramatically excellent bending crashworthiness compared to empty and fully filled square tubes. There exists a foam density threshold, beyond which the CLE of DT-PF achieves a maximum constant. In addition, there seems to be another foam density threshold, beyond which the SEA of DT-PF gets to the maximum value. It is also shown that the foam density threshold corresponding to the maximum SEA varies with the thickness of thin-walled square tubes.

Keywords: thin-walled tube; lightweight foam; bending crashworthiness; energy absorption; finite element analysis
CLC number: O347 **Document code**: A **Article ID**: 1005-9113(2024)00-0000-14

0 Introduction

Thin-walled tubes are widely used in many engineering fields due to their excellent mechanical properties with light weight. Therefore, the thin-walled tubes and related composite structures are extensively applied in both macro- and micro-scaled engineering and technology such as automobile, aerospace, thermal engineering, medicine, environment protection and micro-electro-mechanical technology[1-6]. For example, in terms of buckling of thin-walled tubes that will lead to a disaster, Xu et al.[3] developed a new technology on improving buckling resistance in which the local surface nanocrystallization was adopted to increase the critical loads of thin-walled structures. The optimal design of local surface nanocrystallization was established by estimating the ultimate buckling deformation. In addition to individual thin-walled tubes, the buckling or thermal buckling of micro-thin-walled tubes such as carbon nanotube reinforced composite structures has also received more and more research attention[7]. The research on thin-walled tubes and filled thin-walled tubes has been one of the hotspots over the past several decades[8]. One reason is that they demonstrate an excellent load-carrying capacity and energy-absorbing property as compared with other constructions with identical mass[9-10]. It is well known the bending deformation frequently takes place when a transverse load acts on the engineering structures especially on the thin-walled tubular members[5,8-10]. Kim and Reid[11] first summarized some existing methods of collapse analyses for thin-walled tubes and then developed an admissible and

Received 2024-01-21.
Sponsored by the National Natural Science Foundation of China (Grant Nos. 12272064 and 12101086), the University Natural Science Research Project of Anhui Province (Grant No. KJ2018A0481), the Major Project of Basic Science (Natural Science) Research in Jiangsu Universities (Grant Nos. 22KJA460001, 23KJA580001), the Changzhou Science and Technology Plan Project (Grant No. CE20235049), and the Changzhou Leading Innovative Talents Cultivation Project (Grant No. CQ20220092)
* Corresponding author: Cheng Li, Ph.D, Professor. Email: licheng@czust.edu.cn.

completely analytical solution for bending collapse of thin-walled tubes with a rectangular section, and it agrees well with experimental results reported. Chang et al.[12] showed effects of the mean moment on the response and collapse of circular thin-walled tubes subjected to cyclic bending via both experimental and theoretical approaches, and proposed an empirical formulation to determine the relation between the moment range and the number of cycles necessary to produce buckling for thin-walled tubes since the buckling of thin-walled structures has attracted increasing research interest in recent years. Subsequently, Zhang et al.[13] investigated the bending collapse behaviors of thin-walled square tubes with different thickness for flanges and web plates, and found that placing more materials in the webs and less in flanges is an effective strategy to enhance the bending resistance. Considering the complicated deformation characteristics and influential factors, Huang and Zhang[14] conducted a detailed investigation on the bending collapse of rectangular tubes by both experimental tests and numerical simulations. Bigdeli and Nouri[15] presented systematically the property and optimization of aluminum thin-walled cylindrical energy absorber. The response surface method was adopted and some numerical, experimental and statistical analyses were carried out. Their work implied linear or nonlinear relationships between thickness, height, length and initial peak crushing force and energy absorption per length, respectively. Asanjarani et al.[16] examined the mechanical characteristics and energy absorption behaviors of straight and grooved tapered thin-walled tubes with different cross-section shapes including circle, ellipse, square, rectangle, hexagon, and octagon, and it has shown that mechanical characteristics may be improved via a geometry modification. After that, Jishi et al.[17] paid attention to tubular sandwich structures in which small diameter tubes were fixed onto metallic surface, and then explored their excellent energy-absorbing characteristics, based on which the tubular sandwich structures are expected to be useful in the environment with extreme dynamic loads.

However, the tubes with thin walls are apt to generate local indentation which would largely decrease their global loading capacity. It is more obvious for thin-walled tubes which are subjected to a concentrated force. An effective attempt is filling a lightweight material such as metallic foams into the thin-walled tube to resist the local indentation and keep its global load-carrying capacity[18-20]. Similar ideas can also be used to improve the bending crashworthiness of plates and shells, so as to construct a popular sandwich energy absorption structure[21-24]. Therefore, it is necessary to study the mechanical properties of such a composite structure namely thin-walled tubes filled with metallic foams, including foam filling style, filling amount, design of cross section and so on[25-27]. For example, Santosa et al.[28] examined the bending response of thin-walled square tubes filled with aluminum foams using a nonlinear finite element code, and concluded that the filler restrains inward deformation at a compressive flange. Consequently, it causes a considerable increase of the bending resistance and thus reduces the structural bending deformation. Chen et al.[29] studied the bending collapse of thin-walled square tubes filled with aluminum foams or honeycombs, and derived the moment-rotation relation to optimize the crashworthiness of the filled members. Li and Lu[30] performed a comparative study on the bending crashworthiness characteristics of different tubular structures filled with aluminum foams, and discovered that the energy-absorbing performance of foam-filled double tubes are superior to that of conventional empty or foam-filled single tubes. Gao and Liao[31] designed a novel thin-walled structure filled with double arrowed auxetic members and subsequently revealed its unique mechanical properties especially the energy absorption characteristics. A gradient configuration was proposed and the theoretical model was validated by numerical simulations. Xie et al.[32] presented the bending crashworthiness of thin-walled tubes with multi-cell and double-tube configurations based on the three-point bending simulation.

As aforementioned, filling lightweight materials into thin-walled constructions has been proved to be an efficient way to improve the bending resistance. Nevertheless, lightweight is one of the eternal goals of engineering structures. To furthermore decrease the structural mass, partially filling along the axial direction of the tubes is an effective method. Santosa et al.[28] and Chen et al.[29] found that the thin-walled tubes partially filled with foams show high anti-bending capacity, and the effective filling length is proposed to determine the foam filling length required. However, for the thin-walled tubes partially

filled with foams along the axial direction, the filler would be out of action once the impact acts on the regions without the filler. Moreover, bending behaviors of another kind of partially foam-filled sections named foam-filled double tubes also attract the research attention of some investigators[33]. The results indicated that foam-filled double tubes show higher energy absorbing capacity in comparison with the traditional foam-filled single tubes in the same total mass situation.

Nevertheless, it also needs to be emphasized that this article considers partially filled square tubes. Previous experimental studies have focused on fully filled circular tubes. Due to limitations in specimen preparations and experimental equipments, it is difficult to directly carry out experimental verification in this article. Moreover, there have been few experimental results in previous literature which are completely consistent with the present model for reference. In addition, finite element analysis or simulation has become a commonly used and reliable research method, and the calculation results are also widely adopted in this field.

In the present study, different cross-sectional configurations of thin-walled square tubes partially filled lightweight foams, named DC-PF and DT-PF respectively, are proposed and designed. Subsequently, their bending crashworthiness is examined via a three-point bending test in the framework of the finite element analysis software ABAQUS. Two mechanical indicators CLE and SEA are introduced to show quantitatively the influence mechanism of physical properties of foams on the bending crashworthiness of partially filled thin-walled square tubes. To this end, the empty and fully filled square tubes are used to compare with the analysis results of DC-PF and DT-PF, respectively. The numerical models were established, and three cases of square tubes with the ratios of width to wall thickness b/t = 100, 50, 33 are modeled in detail. Some beneficial numerical results are obtained and discussed. The present research has practical reference significance for the design and optimization of thin-walled tubes partially filled with lightweight metallic foams used in various engineering structures.

1 Structure and Test Designs

Considering a thin-walled square tube with width $b\times b$ and wall thickness t, as shown in Fig. 1(a), it is often fully filled with lightweight foam material to improve load-carrying capacity, as in Fig. 1 (b). When the empty square tube is partitioned by a transverse internal web, they will become a double-cell configuration. Previous research revealed that the inward deformation at the compressive flange is the key to result into the decrease of bending resistance of thin-walled constructions, so it is suggested to only fill the upper cell with lightweight foams, as in Fig. 1(c). In addition, inserting a smaller square tube with width $d\times d$ into the tube and filling the clearing between the two tubes with lightweight foams, the foam-filled double tube comes into being, as demonstrated in Fig. 1(d). All the four configurations are assumed to have the same global width b and the same wall thickness t. Some notations are introduced for the sake of reference convenience. S-E refers to the single empty tube, and S-F represents its counterpart fully filled with lightweight foams. DC-PF and DT-PF denote double-cell tubes and double-tube tubes partially filled with foam, respectively.

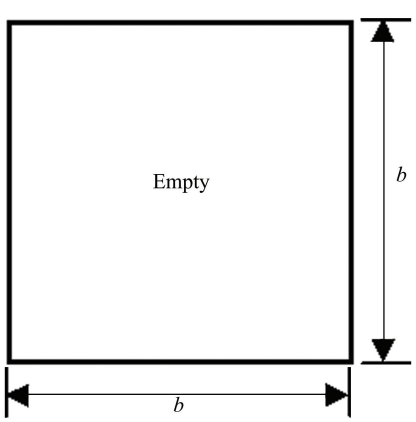

(a) S-E

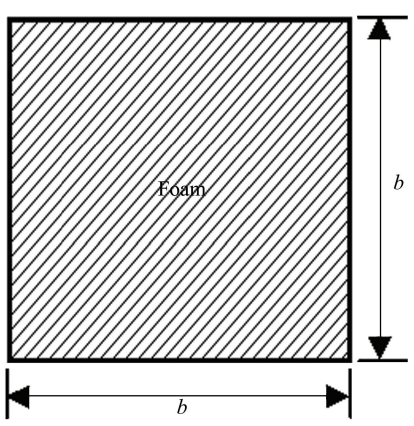

(b) S-F

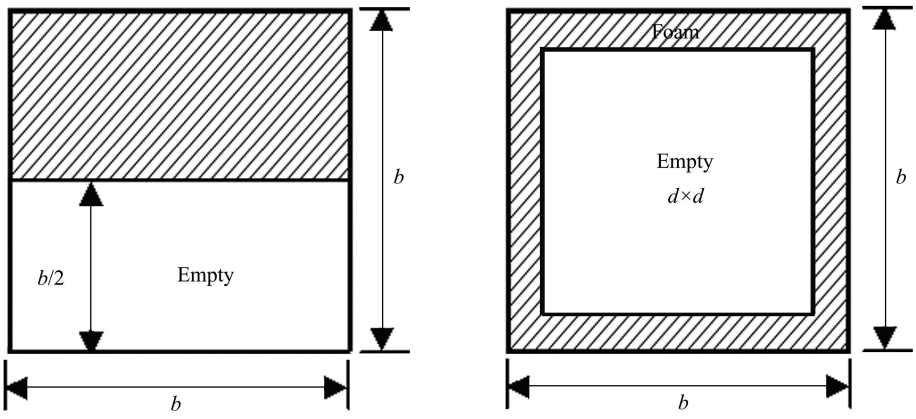

(c) DC-PF (d) DT-PF

Fig. 1 Schematic of the presented cross sections of square tubes

General three-point bending tests of the thin-walled square tubes with the above four cross-sections are suggested for the comparison of bending crashworthiness, as illustrated in Fig.2. The side width of the square cross-section b is assigned 0.1 m, and the two bearings and the loading punch are supposed to be rigid cylinders with identical radius $R = 0.1b = 10$ mm. The whole length of the tubes is $L = 10b = 1$ m, and the span of the tubular beams between the two supports is $s = 8b = 0.8$ m. The tubular walled thickness t is set as 1 mm, 2 mm and 3 mm, which are denoted by $b/t = 100$, 50 and 33, respectively. The internal tube width of DT-PF is assigned a constant value $d = 0.6\ b = 0.06$ m.

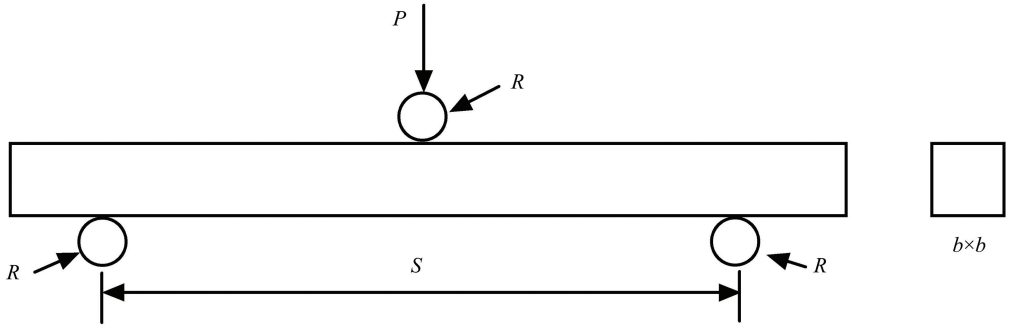

Fig. 2 Schematic of three-point bending tests of thin-walled square tubes

2 Models and Results

2.1 Numerical Models

The finite element code ABAQUS/Explicit is employed to simulate the three-point bending behavior of the four structures mentioned above. Considering the symmetry of the bending tests, a quarter of models are established by assigning symmetric boundary conditions to save the computing time, as represented in Fig. 3.

In the numerical models, the punch and the two bearings are simulated as 3D Analytical Rigid not allowed any deformations, and the thin-walled tubes as 3D deformable shell. The foam fillers are modeled as 3D deformation solid. In addition, the Dynamic, Explicit procedure is executed, and the rigid punch moves downwards at an average velocity 0.1m/s up to a displacement 0.1 m. The interaction between all of the possible contact surfaces is modeled using general contact with frictionless tangential behavior and hard normal behavior. Considering that the structural deformation would occur mainly in a short region across the midspan section, a length 0.3 m of the tubes are more finely meshed with an average size 3 mm, and other region approaching the two ends with 6 mm, as shown in Fig. 3. Similarly, the foams are meshed with sizes 5 mm and 10 mm, respectively. The reliability of the meshing sizes is verified through convergence analysis.

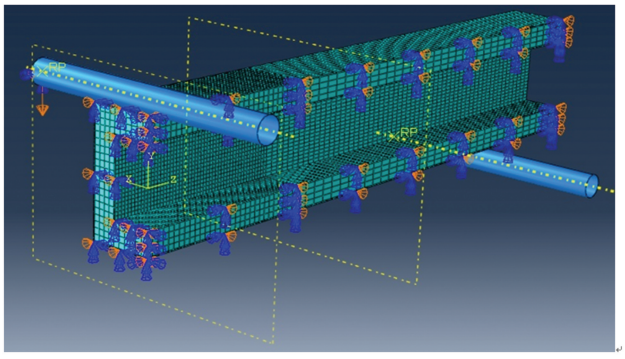

Fig.3 A quarter of numerical model of three-point bending tests for the configuration DT-PF

The tubular walls are assumed to be made of an elastic, ideally plastic metal material with density 7.8×10^3 kg/m^3, elastic modulus E_s = 200 GPa and flow stress $\sigma_{0,s}$ = 600 MPa. The lightweight filler is postulated to be a metallic foam, and its solid cell wall is presumed to be the same as the tubular wall. In the ABAQUS material library, the Crushable Foam model well describes large strain behavior of metallic foams. According to previous studies, mechanical properties of metallic foam could be approximately depicted by Eqs. (1)-(5), where $\bar{\rho}$, E_f, σ_p, $\varepsilon_D^{initial}$ and ε_D^{full} represent its relative density, elastic Young's modulus, plateau stress, initial densification strain, and full densification strain, respectively. Additionally, ρ_f, ρ_s are the density of foam and its solid cell wall material, respectively. The symbols E_s, $\sigma_{0,s}$ refer to the Young's modulus and flow stress of the solid cell wall material.

$$\bar{\rho} = \rho_f/\rho_s \tag{1}$$

$$E_f = E_s\bar{\rho}^2 \tag{2}$$

$$\sigma_p = \sigma_{0,s}\bar{\rho}^{3/2} \tag{3}$$

$$\varepsilon_D^{initial} = 1 - 1.4\bar{\rho} \tag{4}$$

$$\varepsilon_D^{full} = 1 - \bar{\rho} \tag{5}$$

The relations of Eqs. (2) and (4) are obtained from previous research Ref. [34] and Eq. (3) from Ref. [35]. The full densification strain expressed by Eq. (5) means that the foam is fully densified to its solid cell wall material. In the FE models, the nominal stain ε_{nom} under compressive deformation from Eqs. (4) and (5) needs be transformed into the true strain by Eq. (6). Five cases with different foam density are simulated in the present analysis, as shown in Table 1.

$$\varepsilon_{true} = -\ln(1 - \varepsilon_{nom}) \tag{6}$$

On the other hand, three cases of wall thickness t = 1 mm, 2 mm, 3 mm are computed here, and all parameters simulated in the present analysis are summarized in Table 2. For reference convenience, the following notations of the simulated cases are established based on these parameters. For example, S2-E represents the single empty tube with wall thickness 2 mm, and S2-F3 denotes the single tube with wall thickness 2 mm fully filled with the foam with relative density 0.2. DC2-PF3 signifies the double-cell configuration with wall thickness 2 mm partially filled with the foam with relative density 0.2, and so on.

Table 1 The mechanical properties of metallic foams employed in the present analysis

$\bar{\rho}$	ρ_f (kg/m^3)	E_f (MPa)	σ_p (MPa)	$\varepsilon_D^{initial}$		ε_D^{full}	
				ε_{nom}	ε_{true}	ε_{nom}	ε_{true}
0.05	390	500	6.71	0.93	2.659	0.95	2.996
0.1	780	2000	18.97	0.86	1.966	0.90	2.303
0.2	1560	8000	53.67	0.72	1.273	0.80	1.609
0.3	2340	18000	98.59	0.58	0.868	0.70	1.204
0.4	3120	32000	151.79	0.44	0.580	0.60	0.916

Table 2 All parameters simulated in the present analysis

Cross-section	Wall			Metallic foam	
	No.	b/t	Thickness (mm)	No.	$\bar{\rho}$
S-E	1	100	1	1	0.05
S-F	2	50	2	2	0.10
DC-PF	3	33	3	3	0.20
DT-PF				4	0.30
				5	0.40

2.2 Typical Deformation Characteristics

The typical deformation of tubular wall for the above four configurations for the cases S2−E, S2−F3, DC2-PF3, DT2-PF3 is plotted in Fig. 4. It can be seen that S2-E generates large local indentation in a short region under the punch. The large local indentation results in an obvious decrease of the cross-sectional height and bending resistance. When the empty tube is filled with foam material, local indentation is well restrained, and the tubular deformation varies from local indentation to wrinkling. While the empty tube is reinforced with a transverse web and filled with foam material at the upper cell, the global flattening of the cross section and local indentation of the upper cell are both restricted, and load-carrying capacity evidently rises. As the empty tube is reinforced by an internal tube and filled with foam material in the clearing, both the global flattening of the cross section and local indentation of the upper compressive region are controlled, and bending resistance remains high level. It is noted that the external tube of DT-PF demonstrates much similar deformation to that of S-F at the cost of lighter total mass.

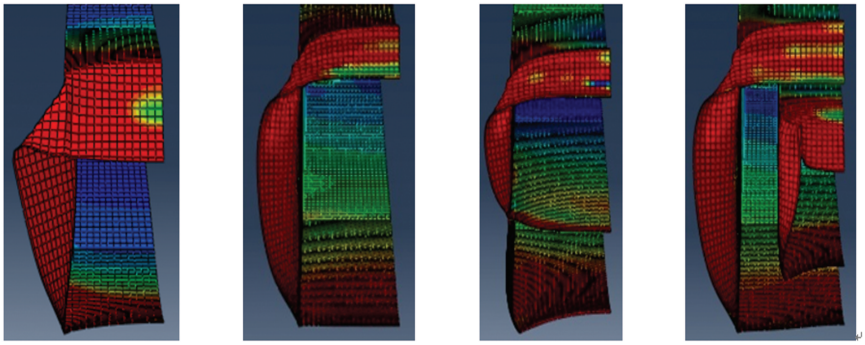

(a) S2-E (b) S2-F3 (c) DC2-PF3 (d) DT2-PF3

Fig. 4 The typical deformation of tubular wall cross-sections at punch displacement 0.1 m

2.3 Punch Forces Versus Displacement

Fig. 5 shows the variation of punch forces with displacement for the case b/t = 100, and wall thickness t = 1 mm. It can be found that the foam filler significantly improves the load-carrying capacity as compared with the corresponding empty tube in Fig.5(a). It is noted that some researchers have carried out experimental research on the simple foam filled thin-walled tubes. For example, Santosa et al.[28] experimentally investigated the bending behaviors of thin-walled columns filled with closed-cell aluminum foam. Chen et al.[29] presented the bending collapse of thin-walled beams filled with aluminum foam or aluminum honeycomb. Hanssen et al.[36] reported an experimental programme for the three-point bending of aluminium extrusions filled with aluminium foam subjected to a quasi-static loading condition. The simulation results obtained in this article are consistent with the experimental results aforementioned in terms of qualitative conclusions. However, compared with existing literature, this study considers a more complex structure, and there are currently no relevant experimental reports considering a configuration that is exactly the same as the one presented in this article termed as a thin-walled square tube partially filled with metallic foams. From Fig.5, when the foam density is smaller, an initial peak force arises after elastic response. For the DC-PF configurations which is obviously an unaxisymmetric structure in finite element analysis, when the foam density is smaller, i.e. $\bar{\rho}$ = 0.05 and 0.1, the force curves run with displacement similar to

the fully filled tubes S-F. It is evidently different when the foam density is larger, i.e. $\bar{\rho}=0.2$, 0.3 and 0.4, the three curves have almost the same initial running trend and subsequently diverge about at displacement 0.4 m. The reason is that large foam density considerably raises sectional bending resistance, the compressing collapse at the lower empty cell upon the two supports precedes the bending collapse under the punch. The compressing collapse at the lower empty cell upon the two supports has little relevance with the foam strength.

For the DT-PF configurations, the force curves display similar tendency but lower lever in comparison with the S-F ones with the same foam density.

As the wall thickness increases, all of the load-carrying capacity increases on the whole but the enhancing effect of the foam fillers descends, see Fig. 6 and Fig. 7. It is noted that the DC2-PF and DC3-PF configurations are dominated by bending collapse under the punch and no obvious compressing collapse at lower empty cell upon the two supports is observed.

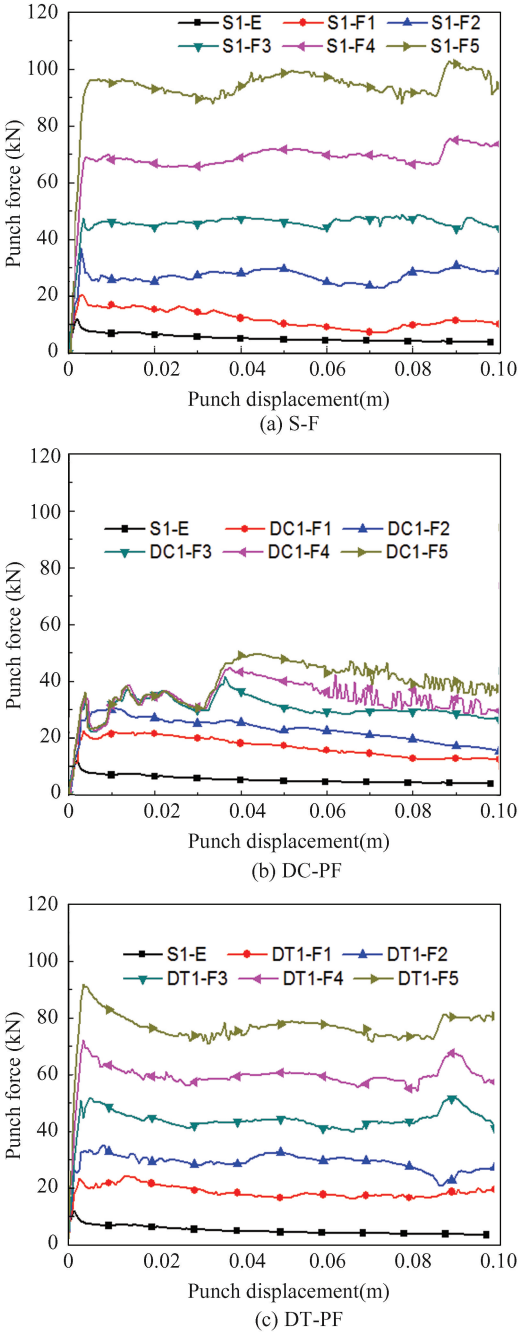

Fig. 5 The variation of the punch forces with displacement for the case b/t = 100

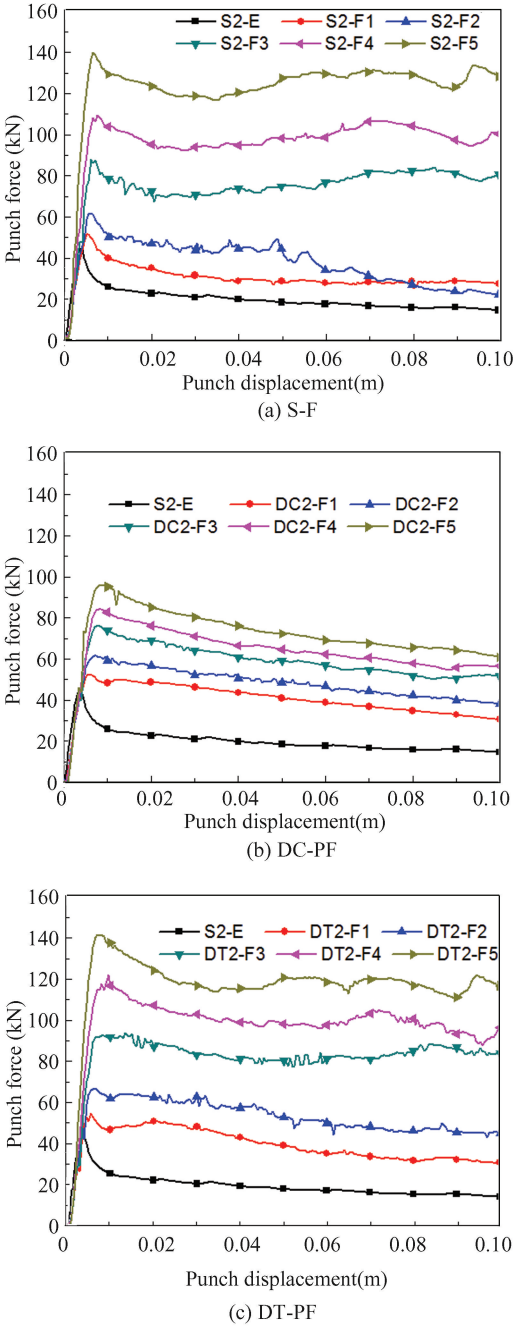

Fig. 6 The variation of the punch forces with displacement for the case b/t = 50

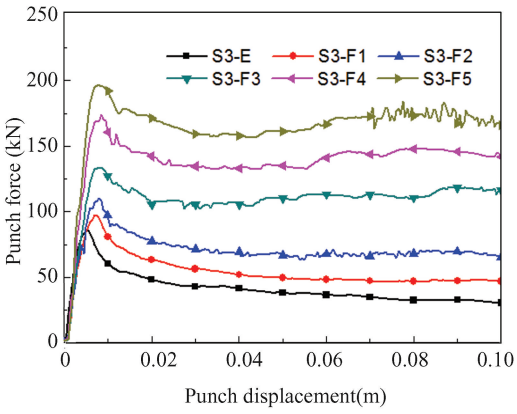

(a) S-F

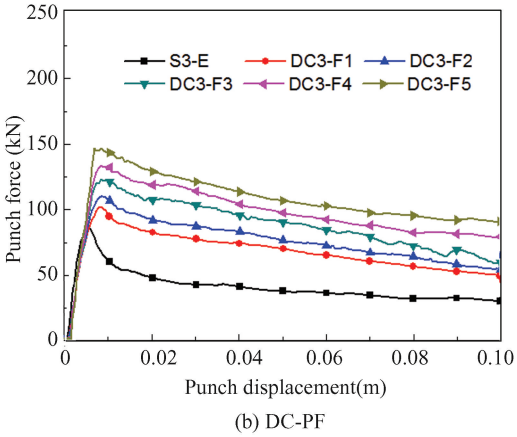

(b) DC-PF

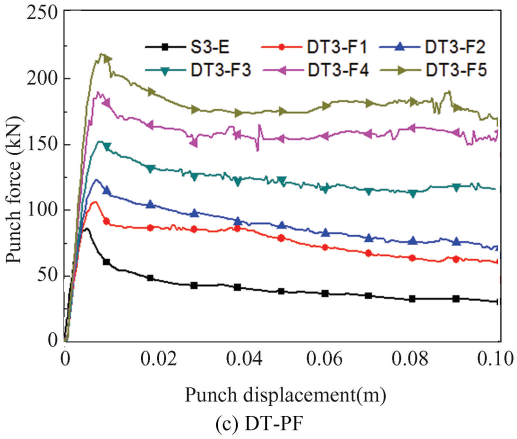

(c) DT-PF

Fig. 7 The variation of the punch forces with displacement for the case b/t = 33

3 Discussion

Energy absorption is an important indicator in some engineering cases. Based on the principle of energy conservation, the structural energy absorption is equal to the work done by the external forces. For the case of three-point bending, only the punch force does work. So, the total energy absorption E_t can be obtained by integrating the punch force P with its displacement δ up to the maximum value δ_{max}, i.e.

$$E_t = \int_0^{\delta_{max}} P\mathrm{d}\delta \tag{7}$$

The mean punch force P_m is another important indicator for an energy absorber, generally defined by the ratio of the total energy absorption E_t to the maximum displacement δ_{max}, as shown in Eq. (8),

$$P_m = E_t/\delta_{max} \tag{8}$$

Moreover, too large peak reaction force perhaps does serious damage to the protected objects for an energy absorber. According to Zarei and Kröger[37], the crash load efficiency CLE is suggested to estimate the impact resistance for a given energy absorption. The definition of the CLE is the ratio of the mean load P_m to the maximum load P_{max} expressed in Eq.(9).

$$\mathrm{CLE} = P_m/P_{max} \tag{9}$$

In addition, it is desired to obtain the maximum energy absorption at the cost of light structure weight in most cases. The specific energy absorption SEA is proposed to evaluate energy absorbing capacity with certain structural mass, defined by the energy absorption per unit mass of the whole structures[38], for example Eq.(10).

$$\mathrm{SEA} = E_t/m_t \tag{10}$$

where m_t is the total mass of the whole structures. For the foam-filled tubes, the total mass is the sum of the mass of tubular wall and that of the foam filler in Eq.(11).

$$m_t = \rho_{wall}A_{wall}L + \rho_{foam}A_{foam}L = (tl_{wall} + \bar{\rho}A_{foam})\rho_{wall}L \tag{11}$$

where L and l_{wall} represent the tubular axial length and the total length of the sectional segments of the tubular wall, respectively. ρ_{wall} is the density of tubular wall material. For the cases S-F, when the foam density equals zero, the above formulation would be reduced to that of the cases S-E.

$$A_c = tl_{wall} + \bar{\rho}A_{foam} \tag{12}$$

where parameter A_c, called characteristic mass here, dominates the total mass. For simplicity, in the following analysis the specific energy absorption SEA is calculated as in Eq.(13).

$$\mathrm{SEA} = E_t/A_c \tag{13}$$

Based on the numerical results as plotted in Figs. 5-7, the calculated results of the above mechanical indicators are listed in Tables 3-5, classified in terms of the parameter b/t.

For intuitive comparison of bending crashworthiness

among the above four configurations, four key mechanical indicators P_{max}, E_t, CLE and SEA are depicted in Figs. 8-11, respectively. Additionally, the indicators of the three configurations S-F, DC-PF and DT-PF are all normalized by that of S-E with the same wall thickness. For example, normalized P_{max} denotes the P_{max} of S-F, DC-PF and DT-PF divided by that of S-E, i.e.

$$\text{Normalized } P_{max} = \frac{P_{max}(\text{S-F, DC-PF, DT-PF})}{P_{max}(\text{S-E})} \quad (14)$$

Table 3 The calculated results of the mechanical indices for the case $b/t = 100$

Specimens	P_{max} (N)	E_t (J)	P_m (N)	A_c (m^2)	SEA (kJ/m^2)	CLE
S1-E	11997	502	5020	0.0004	1255	0.418
S1-F1	20198	1190	11900	0.0009	1322	0.589
S1-F2	37037	2678	26780	0.0014	1913	0.723
S1-F3	48606	4535	45350	0.0024	1890	0.933
S1-F4	75342	6794	67940	0.0034	1998	0.902
S1-F5	102649	9306	93060	0.0044	2115	0.907
DC1-PF1	22536	1661	16610	0.00075	2215	0.737
DC1-PF2	30361	2269	22690	0.001	2269	0.747
DC1-PF3	41738	3044	30440	0.0015	2029	0.729
DC1-PF4	45036	3418	34180	0.002	1709	0.759
DC1-PF5	49784	3908	39080	0.0025	1563	0.785
DT1-PF1	23572	1825	18250	0.00082	2226	0.774
DT1-PF2	34437	2826	28260	0.001	2826	0.821
DT1-PF3	50674	4269	42690	0.00136	3139	0.842
DT1-PF4	70317	5761	57610	0.00172	3349	0.819
DT1-PF5	89402	7405	74050	0.00208	3560	0.828

Table 4 The calculated results of the mechanical indices for the case $b/t = 50$

Specimens	P_{max} (N)	E_t (J)	P_m (N)	A_c (m^2)	SEA (kJ/m^2)	CLE
S2-E	44617	1982	19820	0.0008	2478	0.444
S2-F1	51970	3059	30590	0.0013	2353	0.589
S2-F2	62026	3791	37910	0.0018	2106	0.611
S2-F3	88876	7516	75160	0.0028	2684	0.846
S2-F4	110775	9714	97140	0.0038	2556	0.877
S2-F5	141585	12394	123940	0.0048	2582	0.875
DC2-PF1	52461	4010	40100	0.00125	3208	0.764
DC2-PF2	61590	4740	47400	0.0015	3160	0.770
DC2-PF3	76283	5790	57900	0.002	2895	0.759
DC2-PF4	84078	6374	63740	0.0025	2550	0.758
DC2-PF5	95905	7178	71780	0.003	2393	0.748
DT2-PF1	55031	3952	39520	0.00146	2707	0.718
DT2-PF2	67272	5288	52880	0.00164	3224	0.786
DT2-PF3	94486	8222	82220	0.002	4111	0.870
DT2-PF4	122605	9827	98270	0.00236	4164	0.802
DT2-PF5	141866	11690	116900	0.00272	4298	0.824

Table 5 The calculated results of the mechanical indices for the case b/t = 33

Specimens	P_{max}(N)	E_t(J)	P_m(N)	A_c(m^2)	SEA (kJ/m^2)	CLE
S3-E	86108	4133	41330	0.0012	3444	0.480
S3-F1	97243	5375	53750	0.0017	3162	0.553
S3-F2	109940	7068	70680	0.0022	3213	0.643
S3-F3	133500	10921	109210	0.0032	3413	0.818
S3-F4	174174	13812	138120	0.0042	3289	0.793
S3-F5	196854	16417	164170	0.0052	3157	0.834
DC3-PF1	102149	6808	68080	0.00175	3890	0.666
DC3-PF2	110418	7544	75440	0.002	3772	0.683
DC3−PF3	122956	8707	87070	0.0025	3483	0.708
DC3-PF4	133526	9693	96930	0.003	3231	0.726
DC3-PF5	146907	10673	106730	0.0035	3049	0.727
DT3-PF1	105987	7435	74350	0.0021	3540	0.702
DT3-PF2	122498	8625	86250	0.00228	3783	0.704
DT3-PF3	151145	11815	118150	0.00264	4475	0.782
DT3-PF4	188887	15397	153970	0.003	5132	0.815
DT3-PF5	216774	17475	174750	0.00336	5201	0.806

Regarding the theoretical analyses on bending crashworthiness of thin-walled square tubes partially filled with metallic foams, this article establishes a basic theoretical model with corresponding equations. Additionally, Hanssen et al.[36] developed some design formulae to predict the load bearing capacity of the foam filled beams that can also be referenced.

3.1 P_{max} and E_t

Fig. 8 gives the maximum forces of the foam-filled tubes normalized by that of the single empty tube S-E with identical wall thickness. It can be found that the foam filler largely raises the maximum forces, especially when the wall thickness is small. Furthermore, the maximum forces of the two configurations S-F and DT-PF have similar linear increasing tendency with increasing foam density. However, the DC-PF forces display lower maximum values.

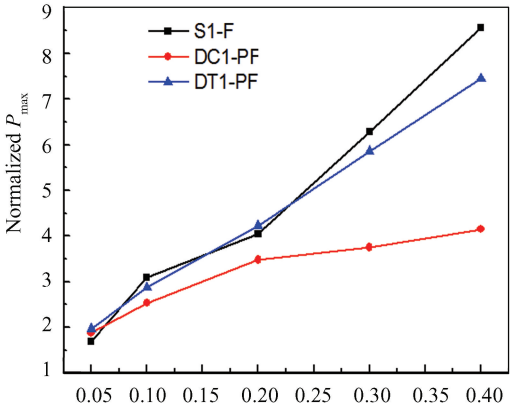

(a) b/t=100

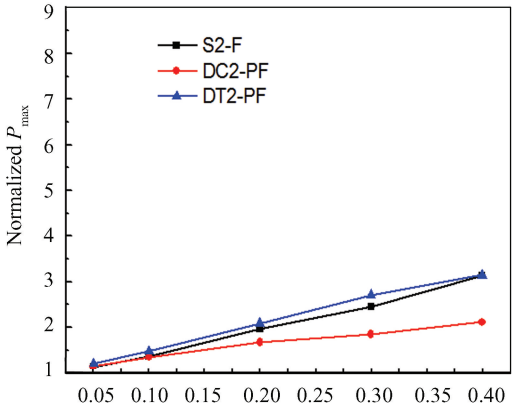

(b) b/t=50

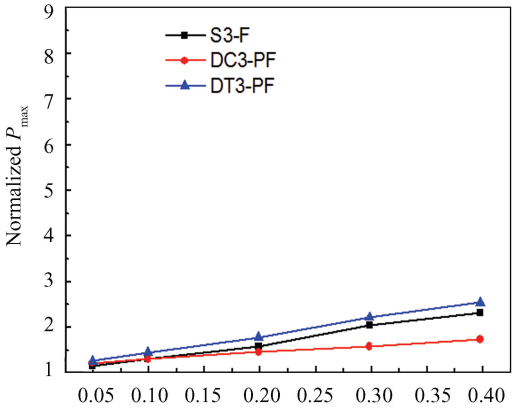

(c) b/t=33

Fig. 8 The maximum forces of the foam-filled tubes normalized by that of the single empty tube S-E for the different cases

On the whole, the total energy absorption demonstrates similar variational characteristics to the maximum forces, as shown in Fig. 9. The two configurations S-F and DT-PF exhibit higher energy absorbing capacity than DC-PF when the relative density of foam filler is larger than about 0.1.

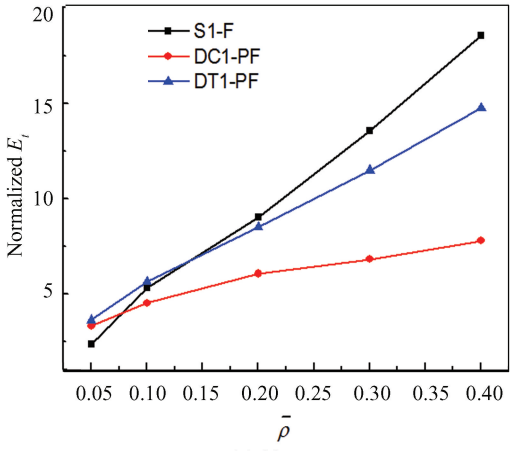

(a) b/t=100

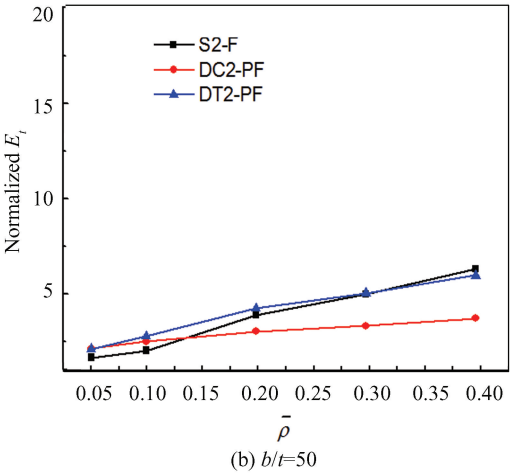

(b) b/t=50

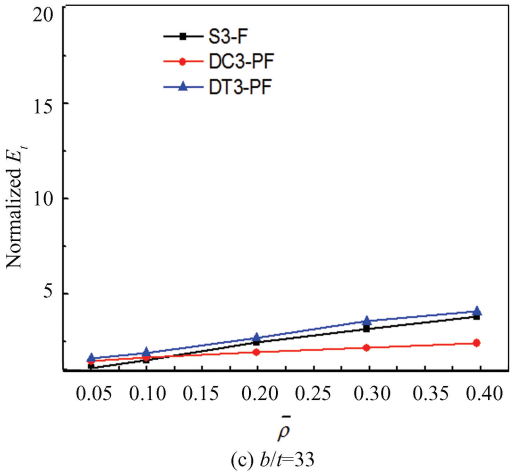

(c) b/t=33

Fig. 9 The total energy absorption of the foam-filled tubes normalized by that of the single empty tube S-E for the different cases

3.2 CLE and SEA

Fig. 10 presents the variation of the CLE of foam-filled tubes normalized by that of the single empty tube S-E with the same wall thickness. It can be observed that the CLE of the three foam-filled configurations is prominently larger than that of the configuration S-E, especially when the wall thickness is small. The CLE of the configurations S-F ascends with the relative density of foam filler till it arrives at 0.2. When the relative density of foam filler extends to 0.2, the CLE of S-F almost keeps stable. For the case b/t = 100, the CLE of the two configurations DC-PF and DT-PF is larger than that of S-F when the foam density is small. On the contrary, the CLE of DC-PF and DT-PF is smaller than that of S-F. What's more, the CLE of DT-PF is greater than that of DC-PF. With the increase of wall thickness, the difference of the CLE among the three configurations becomes smaller. It is noted that the CLE of DT-PF keeps approximately stable when the relative density of the foam filler is larger than 0.2. There seems to exist a constant foam density threshold, beyond which the CLE of DT-PF achieves a maximum constant value.

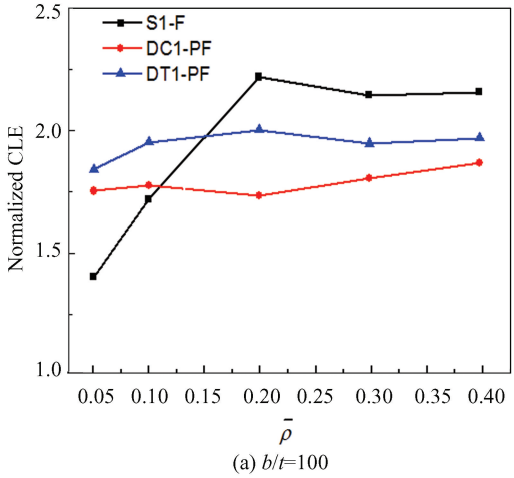

(a) b/t=100

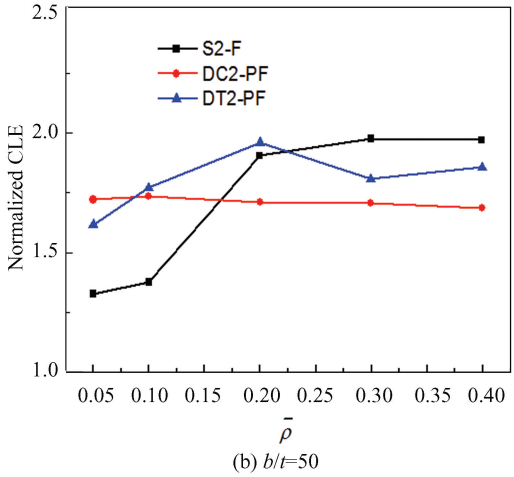

(b) b/t=50

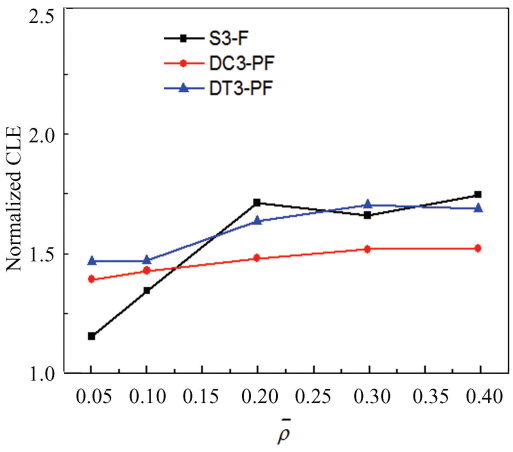

(c) b/t=33

Fig. 10 The CLE of the foam-filled tubes normalized by that of the single empty tube S-E for the different cases

Fig.11 demonstrates the variation of the SEA of the foam-filled tubes normalized by that of the single empty tube S-E with identical wall thickness. It can be seen that when the wall thickness is small, i.e. b/t = 100, the SEA of S-F is remarkably larger than that of S-E. While the wall thickness is larger, i.e. b/t = 50, 33, the SEA of S-F is almost identical to that of S-E. The SEA of DC-PF Linearty decreases. The SEA of DT-PF extends considerably beyond the SEA of S-F and DC-PF, especially when the wall thickness is small. Moreover, the SEA of DT-PF remains approximately constant, when the foam density is greater than 0.1, 0.2 and 0.3 for the case b/t = 100, 50 and 33 respectively. There seems to be a foam density threshold, beyond which the SEA of DT-PF achieves a maximum constant value. However, the foam density threshold corresponding to the maximum SEA varies with the wall thickness.

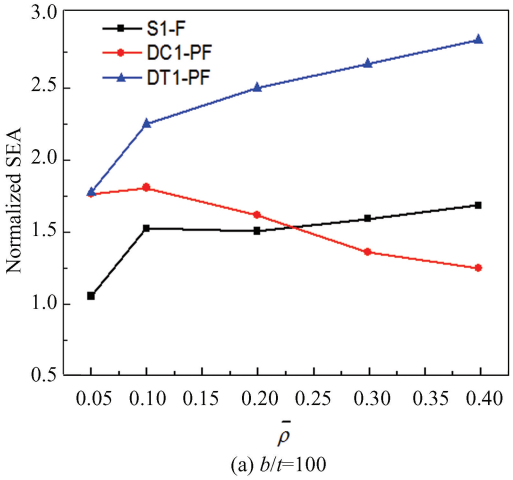

(a) b/t=100

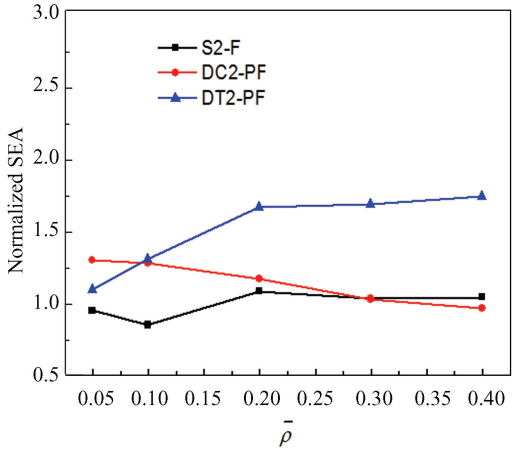

(b) b/t=50

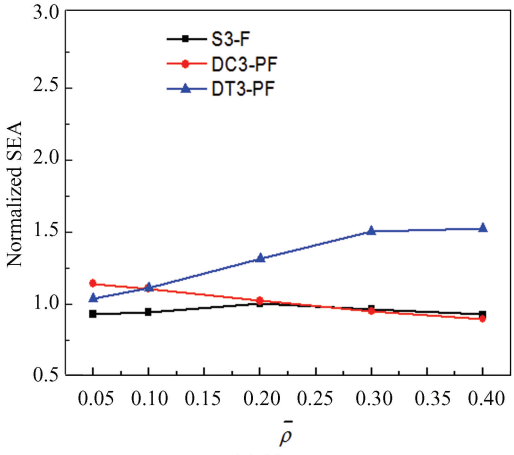

(c) b/t=33

Fig. 11 The SEA of the foam-filled tubes normalized by that of the single empty tube S-E for different cases

4 Conclusions

This work is concerned with the thin-walled tubes which are commonly seen in practical engineering. The main attention is focused on the bending crashworthiness of thin-walled square tubes partially filled with metallic foams. The three-point bending behavior is simulated by employing the finite element ABAQUS/Explicit code, and three cases with the ratio of tube width to wall thickness b/t = 100, 50, 33 are modeled, respectively. The bending crashworthiness of two configurations named DC-PF and DT-PF designed in the present study is examined using two key indicators CLE and SEA, and the corresponding results of empty and fully filled tubes are also presented to indicate the superiority of partially filled tubes over others. The numerical results show that the two configurations especially DT-PF

reveals excellent bending crashworthiness. In addition, the CLE of DT-PF keeps approximately constant when the relative density of the foam filler is larger than 0.2. There is a threshold for the foam density, beyond which the CLE of DT-PF receives a peak value. Moreover, the SEA of DT-PF remains approximately a constant, when the foam density is greater than 0.1, 0.2 and 0.3 for the case b/t = 100, 50 and 33 respectively. There exists another density threshold, and the SEA of DT-PF arrives at a maximum when the threshold is exceeded. However, the foam density threshold related to the maximum SEA is not static, which changes with respect to the wall thickness. The main contribution of the research is to propose the DC-PF and DT-PF configurations of thin-walled square tubes partially filled with metallic foams and demonstrate their advantages in the bending crashworthiness.

References

[1] Wen T, Chen X. Investigation of guided external inversion of thin-walled round tube. Journal of Harbin Institute of Technology (New Series), 2012, 19(3): 38-42.

[2] Wang H, Tang Y, Liu Z, et al. Machining deformation prediction of thin-walled part based on finite element analysis. Journal of Harbin Institute of Technology (New Series), 2015, 22(4): 47-54. DOI: 10.11916/j.issn.1005-9113.2015.04.006.

[3] Xu X, Zhao Z, Zhou Z, et al. Local surface nanocrystallization for buckling-resistant thin-walled structures. International of Journal of Mechanics and Materials in Desigh, 2020, 16: 693-705. DOI: 10.1007/s10999-020-09497-8.

[4] Hu W P, Huai Y L, Xu M B, et al. Mechanoelectrical flexible hub-beam model of ionic-type solvent-free nanofluids. Mechanical Systems and Signal Processing, 2021, 159: 107833. DOI: 10.1016/j.ymssp.2021.107833.

[5] Sebaey T A, Rajak D K, Mehboob H. Internally stiffened foam-filled carbon fiber reinforced composite tubes under impact loading for energy absorption applications. Composite Structures, 2021, 255: 112910. DOI: 10.1016/j.compstruct.2020.112910.

[6] Yan J, Yi S, Yuan X. Graphene and its composites: A review of recent advances and applications in logistics transportation. Packaging Technology Science, 2024, 37(4): 335-361. DOI: 10.1002/pts.2795.

[7] Li C, Zhu C X, Lim C W, et al. Nonlinear in-plane thermal buckling of rotationally restrained functionally graded carbon nanotube reinforced composite shallow arches under uniform radial loading. Applied Mathematics and Mechanics, 2022, 43 (12): 1821-1840. DOI: 10.1007/s10483-022-2917-7.

[8] Lv J Y, Bai Z H, Du X P, et al. Crashworthiness design of 3D lattice-structure filled thin-walled tubes based on data mining. International Journal of Crashworthiness, 2023, 28 (3): 435-448. DOI: 10.1080/13588265.2022.2101306.

[9] Xu X S, Zhao Z, Wang W, et al. A novel design of thin-walled energy absorption structures with local surface nanocrystallization. thin-walled Structures, 2021, 160: 107337. DOI: 10.1016/j.tws.2020.107337.

[10] Zhang H, Chang B X, Peng K F, et al. Anti-blast analysis and design of a sacrificial cladding with graded foam-filled tubes. thin-walled Structures, 2023, 182: 110313. DOI: 10.1016/j.tws.2022.110313.

[11] Kim T H, Reid S R. Bending collapse of thin-walled rectangular section columns. Computers & Structures, 2001, 79 (20-21): 1897-1911. DOI: 10.1016/S0045-7949(01)00089-X.

[12] Chang K H, Pan W F, Lee K L. Mean moment effect on circular thin-walled tubes under cyclic bending. Structural Engineering and Mechanics, 2008, 28 (5): 495-514. DOI: 10.12989/sem.2008.28.5.495.

[13] Zhang X, Zhang H, Wang Z, Bending collapse of square tubes with variable thickness. International Journal of Mechanical Sciences, 2016, 106: 107-116. DOI: 10.1016/j.ijmecsci.2015.12.006.

[14] Huang Z X, Zhang X. Three-point bending collapse of thin-walled rectangular beams. International Journal of Mechanical Sciences, 2018, 144: 461-479. DOI: 10.1016/j.ijmecsci.2018.06.001.

[15] Bigdeli A, Nouri M D. Investigation of the numerical, experimental, statistical and optimization of thin-walled energy absorber with novel configuration using response surface method under axial loading. Journal of Sandwich Structures & Materials, 2020, 22 (8): 2735-2767. DOI: 10.1177/1099636218813196.

[16] Asanjarani A, Mahdian A, Dibajian S H. Comparative analysis of energy absorption behavior of tapered and grooved thin-walled tubes with the various geometry of the cross section. Mech Adv Matl Struct, 2020, 27 (8): 633-644. DOI: 10.1080/15376494.2018.1488311.

[17] Jishi H Z, Alia R A, Cantwell W J. The energy-absorbing characteristics of tubular sandwich structures. Journal of Sandwich Structures & Materials, 2022, 24 (1): 742-762. DOI: 10.1177/10996362211020457.

[18] Jamsari M A, Kueh C, Gray-Stuart E M, et al. Modelling the impact of crushing on the strength performance of corrugated fibreboard. Packaging Technology Science, 2020, 33 (4-5): 159-170. DOI: 10.1002/pts.2494.

[19] Zhao Y J, Cao Y F, Li L Y, et al. Experimental and finite element simulation study of the mechanical behaviors of aluminum foam-filled single/double tubes. Materials Research Express, 2023, 10 (4): 046506. DOI: 10.1088/2053-1591/acc2a4.

[20] Altin M, Arici S. Investigation of the crushing performance of bio-inspired structure filled thin-walled

hybrid aluminum tubes under axial loadings. Journal of the Faculty of Engineering and Architecture of Gazi University, 2024, 39 (2): 1303-1313. DOI: 10.17341/gazimmfd.1287380.

[21] Stapleton S E, Adams D O. Core design for energy absorption in sandwich composites. Journal of Composite Materials, 2009, 43 (2): 175-190. DOI: 10.1177/0021998308099225.

[22] Hou X H, Deng Z C, Zhang K. Dynamic crushing strength analysis of auxetic honeycombs. Acta Mechanica Solida Sinica, 2016, 29 (5): 490-501. DOI: 10.1016/S0894-9166(16)30267-1.

[23] Bodaghi M, Serjouei A, Zolfagharian A, et al. Reversible energy absorbing meta-sandwiches by FDM 4D printing. International Journal of Mechanical Sciences, 2020, 173: 105451. DOI: 10.1016/j.ijmecsci.2020.105451.

[24] Khaire N, Tiwari G, Iqbal M A. Energy absorption characteristic of sandwich shell structure against conical and hemispherical nose projectile. Composite Structures, 2021, 258: 113396. DOI: 10.1016/j.compstruct.2020.113396.

[25] Hou S J, Li Q, Long S Y, et al. Crashworthiness design for foam filled thin-wall structures. Materials Q. Design, 2009, 30 (6): 2024-2032. DOI: 10.1016/j.matdes.2008.08.044.

[26] Rogala M, Ferdynus M, Gawdzinska K, et al. The influence of different length aluminum foam filling on mechanical behavior of a square thin-walled column. Materials, 2021, 14 (13): 3630. DOI: 10.3390/ma14133630.

[27] Ou X, Yao X H, Zhang R, et al. Nonlinear dynamic response analysis of cylindrical composite stiffened laminates based on the weak form quadrature element method. Composite Structures, 2018, 203: 446-457. DOI: 10.1016/j.compstruct.2018.06.114.

[28] Santosa S, Banhart J, Wierzbicki T. Experimental and numerical analyses of bending of foam-filled sections. Acta Mechanica, 2001, 148: 199-213. DOI: 10.1007/BF01183678.

[29] Chen W, Wierzbicki T, Santosa S. Bending collapse of thin-walled beams with ultralight filler: Numerical simulation and weight optimization. Acta Mechanica, 2002, 153: 183-206. DOI: 10.1007/BF01177451.

[30] Li Z B, Lu F Y. Bending resistance and energy-absorbing effectiveness of empty and foam-filled thin-walled tubes. Journal of Reinforced Plastics and Composites, 2015, 34(9):761-768. DOI: 10.1177/0731684415580329.

[31] Gao Q, Liao W H. Energy absorption of thin walled tube filled with gradient auxetic structures-theory and simulation. International Journal of Mechanical Sciences, 2021, 201: 106475. DOI: 10.1016/j.ijmecsci.2021.106475.

[32] Xie Z X, Zhao Z X, Li C. Bending crashworthiness of thin-walled square tubes with multi-cell and double-tube cross-sections. Journal of Mechanical Science and Technology, 2021, 35 (11): 4815-4823. DOI: 10.1007/s12206-021-1001-6.

[33] Guo L W, Yu J L. Dynamic bending response of double cylindrical tubes filled with aluminum foam. International Journal of Impact Engineering, 2011, 38: 85-94. DOI: 10.1016/j.ijimpeng.2010.10.004.

[34] Gibson L J, Ashby M F. Cellular Solids: Structure and Properties. Cambridge: Cambridge University Press, 1997. DOI: 10.1017/CBO9781139878326.

[35] Santosa S, Wierzbicki T. On the modeling of crush behavior of a closed-cell aluminum foam structure. Journal of Mechanics and Physics, 1998, 46 (4): 645-669. DOI: 10.1016/S0022-5096(97)00082-3.

[36] Hanssen A G, Hopperstad O S, Langseth M. Bending of square aluminium extrusions with aluminium foam filler. Acta Mechanica, 2000, 142: 13-31. DOI: 10.1007/BF01190010.

[37] Zarei H R, Kröger M. Crashworthiness optimization of empty and filled aluminum crash boxes. International Journal of Crashworthiness, 2007, 12 (3): 255-264. DOI: 10.1080/13588260701441159.

[38] Kim H S. New extruded multi-cell aluminum profile for maximum crash energy absorption and weight efficiency. Thin-Walled Structures, 2002, 40 (4): 311-327. DOI: 10.1016/S0263-8231(01)00069-6.